ISSN 1 746-7233, England, UK
World Journal of Modelling and Simulation
Vol. 12 (2016) No. 4, pp. 292-306

Analysis of interior permanent magnet synchronous motor with modified direct torque control using fuzzy logic controller

N. Krishna Kumari[1*], G, Tulasiram Das[2], M. P. Soni[3]

[1] Department of Electrical and Electronics Engineering, VNR VJIET, Hyderabad, A. P., India
[2] Professor, EEE Department, Jawaharlal Nehru Technological University, Hyderabad, A. P., India
[3] Professor, EEE Department, MJCET, Hyderabad, A. P., India

(*Received November 12 2014, Accepted July 17 2016*)

Abstract. This paper deals with the novel modified direct torque control (MDTC) scheme based on space vector modulation for an interior permanent magnet synchronous motor(IPMSM) drive. Space vector modulation is used to find the optimal switching sequence of the inverter with respect to torque and flux demand of the drive. The complete system is modelled using Matlab/ Simulink. In the proposed MDTC, the torque and flux ripples are minimised using PI and Fuzzy Logic Controllers. The comparative results show that the Fuzzy Logic Control (FLC) adopted here is more robust. In both the controllers the speed momentarily follows with load disturbances and immediately within no time reaches to the reference value. Also it is observed from performance indices analysis the torque and flux errors are less with fuzzy logic controller and, hence, found to be a suitable replacement of the PI controller for the high performance industrial drive applications.

Keywords: fuzzy logic control (FLC), PI Controller, permanent magnet synchronous motor (PMSM), space vector modulation (SVM) , MDTC, performance indices

1 Introduction

PMSM Drives have been a topic of interest for the last twenty years. These motors are the best choice in drive applications where the drive requires fast and accurate torque response for example servo drives[6].

Due to the enhancement of magnet materials and manufacturing techniques, this machine is mostly suitable for high-precision in position control applications, high performance, variable speed drives due to their maximum torque capability[19, 27].

The necessity of energy saving has lead the industrial interest to the efficient motors. The key efforts for higher efficient motors are paying attention on the development of materials and optimization of design approaches[11]. The advantages of having high power factor, torque density, efficiency and absence of the excitation winding[16] made PMSMs more competitive over induction motors[11].

Also high-performance PMSMs which makes use of surface-mounted magnets on a rotor has large air gap. This feature ensures minimum armature effect on the rotor magnetic field from stator so that the cogging torque and reluctance torque effects are minimized[5, 6, 25]. The flux-weakening operation with adequate torque ability of Surface mounted permanent synchronous motors (SPMs) finds applications in wind generators and spindle drives in attaining a wide range of speed control[4, 9, 10]. The absence of rotor winding and its related losses results in high efficiency, high torque/ weight ratio and reduced cooling arrangements[23]. Due to these features, in contrast to electromagnetic excitation machines PMSM possesses lack of sliding contacts and high energy density per unit volume[22].

The development of cost effective permanent magnet materials like Sm-Co and Nd-Fe-B and modern power electronics made it possible for efficient and compact size PMSMs in applications such as automotive,

* Corresponding author. *E-mail address*: nkkpsg@gmail.com

aeronautical, servo drives, robotics and high precision low cost positioning systems[17, 18, 27]. These applications require low inertia motors, more torque to volume and more torque to current ratio[2]. PMSMs are more efficient in HEV traction drives where in it requires constant power over a wide range of speed without affecting the efficiency and performance of the system[31]. SPMs with distributed windings are used in these applications[15]. Also PMSMs are increasing their popularity in railway industry due to its low maintenance, compact size, less weight, simple structure high torque density, better power factor and high efficiency[1]. Hence having feasibility of using it as a totally enclosed motor it is very well suited for traction applications[14]. Also due to its feature like generation of low acoustic noise compared to other AC drives this motor is suitable in sea and submarine vehicles[14]. In automation control fields as an actuators and robotics due to their superior power density [8].

Two important principle methods are recommended for the dynamic performance of AC drives. The first method, vector control was introduced in 1960's. In this method, the stator current is divided in to torque and flux producing component by using the direction of rotating rotor flux as a reference vector[3]. The second method, Direct Torque Control was introduced in 1984 by M. Depenbrock and in 1986 by I. Takahashi and T. Noguchi. Comparison between Field Oriented Control (FOC) and DTC[7].

Both methods gives a high performance with faster torque dynamics during transient state using DTC and while superior steady-state using FOC[13]. After 1990s, implementation of DTC for interior permanent magnet synchronous machine (IPM) was initiated[6, 21, 30]. It was originated from the DTC of Induction motor in 1980's[20].PMSM with DTC are preferred in applications where it requires fast torque response and high performance operation[30].

The DTC is a sensor less technique and it requires only the initial position of the rotor[29]. The continuous rotor position necessary for torque control is not required in DTC, if the initial rotor position is known unlike in the vector control scheme. All these features make the low-cost sensor less for interior permanent magnet synchronous machine (IPM) drives easier to be implemented, compared with vector control[21].

In case of non linear systems, such as DTC these conventional controllers do not give automatic control because of the non availability of pre defined sets. In such cases, FLC is a better choice for non linear systems to achieve automatic control of plant parameters. In a FLC, the plant parameters are in tune by a fuzzy rule based scheme, which is a logical model of the expert's knowledge for a plant control.

The key feature of a DTC is its exact control and quick response. Hence correct voltage space vector with a smaller hysteresis band is possible by choosing appropriate membership functions and rule base in FLC which reduces torque and flux ripples to a great amount. The design of a PI and FLCs are explained in the following sub sequent sections.

The implementation of a FLC is mainly based on Fuzzy set theory which was introduced by[23, 28]. The main feature of fuzzy systems is that it transforms expert knowledge in to a mathematical formula. Unlike conventional controllers, fuzzy controllers are designed on the basis of heuristics and human experience. FLC converts a set of natural linguistic variables into a automatic control method with expert knowledge[12, 24].

The proposed work in this paper deals with novel and simple MDTC for minimising the flux and torque ripple in IPMSM.

Adopting MDTC which is proposed in this paper, the magnitude of torque and flux ripples can be minimized when compared to that of DTC[26].The detailed MDTC fed IPMSM with PI, Fuzzy controller is modelled in Matlab/ Simulink, results show that torque and flux ripples are greatly reduced using fuzzy controller when compaered to PI Controller.

2 DTC with space vector division

DTC controls the torque and speed of a motor based on the status of the electromagnetic torque as similar to separately excited DC Motor. It not only controls the torque and flux of the motor but also ensures optimum switching losses using proper stator voltage vector. Fig. 1 shows the general DTC block diagram. It has flux and torque hysteresis controllers. These controllers enhance the command values under all load conditions. DTC does not require any current control loop to control the stator flux linkage and the torque. Here the control of the flux and torque is possible by using hysteresis comparators and selecting corresponding voltage

vector from a pre defined switching table. But the amount of ripples associated with the torque and flux are more in this general DTC method. This drawback could be overcome by adopting MDTC with PI and fuzzy logic controllers.

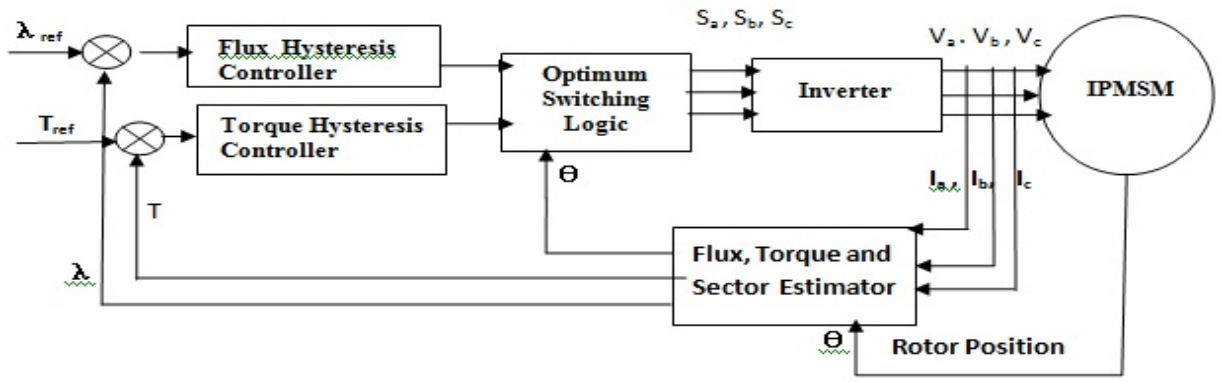

Fig. 1: General block diagram of the DTC

Table 1: Space Vector Division

Sector No.	Modified DTC (DTC1)	DTC II	Conventional DTC (DTC III)
1	$0° \rightarrow 60°$	$-45° \rightarrow 15°$	$-30° \rightarrow +30°$
2	$60° \rightarrow 120°$	$15° \rightarrow 75°$	$+30° \rightarrow 90°$
3	$120° \rightarrow 180°$	$75° \rightarrow 135°$	$90° \rightarrow 150°$
4	$180° \rightarrow 240°$	$135° \rightarrow 195°$	$150° \rightarrow 2100°$
5	$240° \rightarrow 300°$	$195° \rightarrow 255°$	$210° \rightarrow 270°$
6	$300° \rightarrow 360°$	$255° \rightarrow 315°$	$270° \rightarrow 330°$

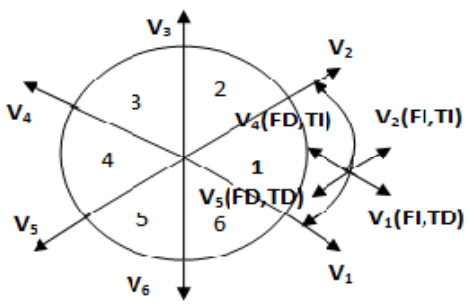

Fig. 2: Voltage vector selection for DTC III

3 Modelling of IPMSM

The complete system comprises of actual motor model, adaptive motor model, flux hysteresis controller, torque hysteresis controller, PI controller, Fuzzy controller, optimal switching logic and inverter which are represented by mathematical equations as described below. The simulation block diagram of MDTC IPMSM is shown in Fig. 3.

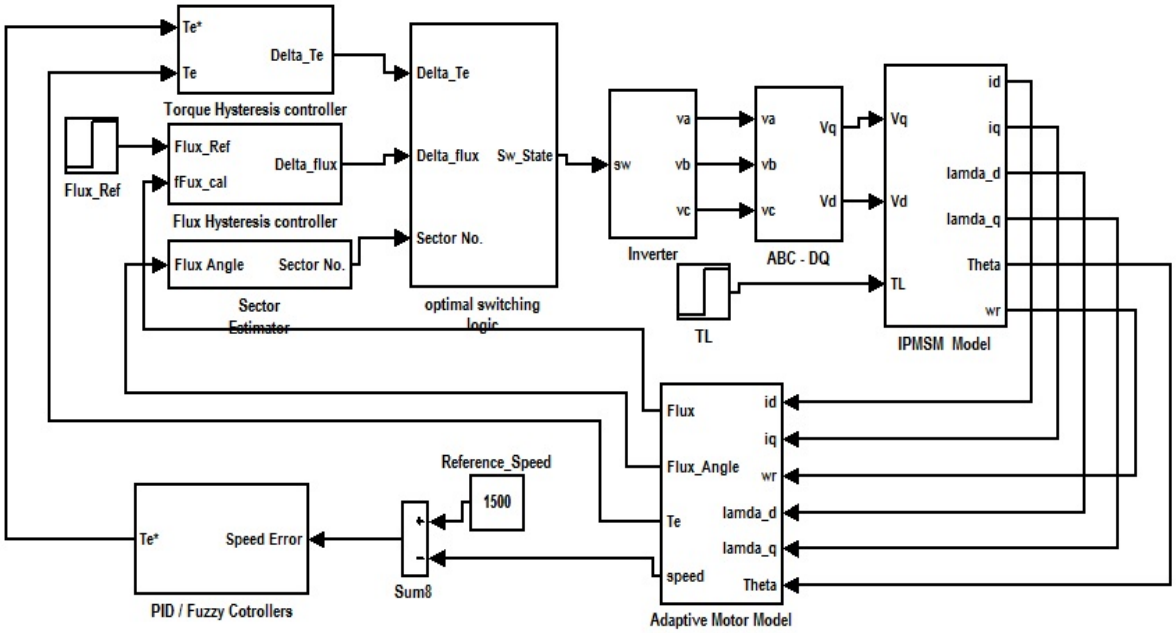

Fig. 3: Simulation block diagram of MDTC IPMSM

3.1 Actual motor model

An accurate dynamic model of the motor is necessary which can explain the dynamic behavior of the machine under both transient and steady state conditions.. In the rotor reference frame, the voltage equation and the torque equation of IPMSM are expressed as follows[30].

$$V_d = R_s i_d + L_d \frac{di_d}{dt} - (\omega_r) L_q i_q, \tag{1}$$

$$V_q = R_s i_q + L_q \frac{di_q}{dt} + (\omega_r) L_d i_d + (\omega_r) \lambda_f, \tag{2}$$

$$\lambda_d = L_d i_d + \lambda_f, \tag{3}$$

$$\lambda_q = L_q i_q, \tag{4}$$

$$T_e = \frac{3}{2}\frac{P}{2}[L_d i_q i_d + \lambda_f i_q - L_q i_q i_d], \tag{5}$$

where R_s is stator armature resistance (Ω), L_d, L_q are direct and quadrature inductances (H), ω_r is rotor speed in electrical (rad/s) T_ε is electromagnetic torque (Nm), P is no. Of poles, λ_f is magnetic flux linkage (wb). As indicated in [25], stable torque control can be achieved if

$$\lambda_s \leq \frac{L_q}{L_q - L_d}. \tag{6}$$

3.2 Adaptive motor model

Adaptive motor model is designed to generate four internal feedback signals namely stator flux (λ), electromagnetic torque (Te), rotor speed (ω), phaser angle between stator flux linkage (θ). The equations are given below.

$$\lambda = \sqrt{\lambda_d 2 + \lambda_q 2}, \tag{7}$$

$$T_e - T_L = \tfrac{2}{p} J \tfrac{d\omega_r}{dt}, \tag{8}$$

$$\theta = Tan^{-1}\left[\frac{\lambda_{qs}}{\lambda_{ds}}\right], \tag{9}$$

where T_L = Load torque in Nm, J = Moment of inertia in Kg·m^2.

3.3 Flux hysteresis controller

The two level hysteresis block is realized using a relay block. The output S takes the value 0 or 1 according to the equations given below. If $|\psi_{s-ref}| - |\psi_{s-est}| \rangle \frac{\Delta\psi_s}{2}$, then the output of the flux controller $S_\lambda = 1$ i.e. it commands to increase the flux magnitude. If $|\psi_{s-ref}| - |\psi_{s-est}| \langle -\frac{\Delta\psi_s}{2}$, then the output of the flux controller $S_\lambda = 0$ i.e. it commands to decrease the flux magnitude. The simulink block diagram for flux hysteresis controller is shown in Fig. 4.

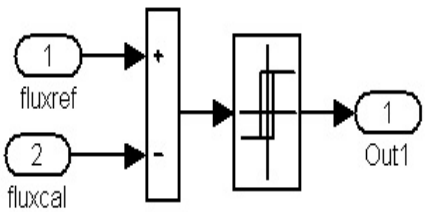

Fig. 4: Simulink Block Diagram for Flux Hysteresis Controller

3.4 Torque hysteresis controller

The three level torque controller has two switch blocks, which represents the hysteresis band for both positive and negative values of torque reference. The output takes values 1 or -1 or 0.

i) If $(T_{ref} - T_e) > \Delta T_e$ then $S_T = 1$, i.e. increase / decrease the torque by switching the states so that it accelerates / decelerates the in counter clockwise /clockwise direction respectively.
ii) If $-\Delta T_e < (T_{ref} - T_e) < \Delta T_e$, then $S_T = 0$ i.e. reduces the torque by switching the zero states.
iii) If $(T_{ref} - T_e) - T_e$ then $S_T = -1$, i.e. decrease / increase the torque by switching the states so that it decelerates / accelerates the in counter clockwise / clockwise direction respectively. The simulink block diagram of torque hysteresis controller is shown in Fig. 5.

Hysteresis band is an important factor in both flux and torque hysteresis controllers, Because a too small value looses the control action in these controllers. A narrow hysteresis band will give better current and flux waveforms but it will increase the inverter switching frequency.

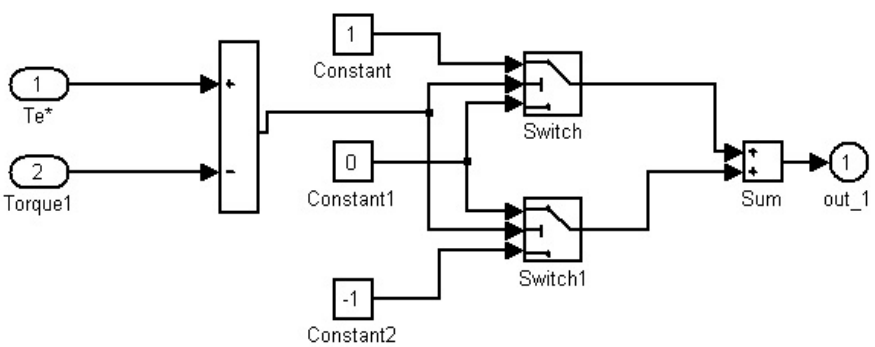

Fig. 5: Simulink block diagram for torque hysteresis controller

3.5 Optimal switching logic

Optimal switching logic processes the instantaneous torque status output and the flux status output by taking the out puts from hysteresis controllers, the corresponding look up table for all its six sectors is given in Tab. 2 , which is formed by using the conditions mentioned in Tab. 3. By using switching functions S_a, S_b and S_c of which value is either 1 or 0, the primary voltage vector is represented as (IsaoTakahashi1986)

$$v\left(S_a, S_b, S_c\right) = \sqrt{\frac{2}{3}} V_{dc}\left[S_a + S_b \exp\left(j\frac{2\pi}{3}\right) + S_c \exp\left(j\frac{4\pi}{3}\right)\right]. \tag{10}$$

3.6 Voltage source inverter (VSI)

The stator flux is controlled by proper selection of voltage vectors, higher the speed of stator flux rotation the faster the torque response. In a MDTC scheme it is possible to construct the voltage vector from the DC link voltage and the switching states (S_a, S_b, S_c) of a VSI. The primary voltage vector V_s is defined by the following Eq. (10).

Table 2: Switching table for MDTC

Sector No. $(\theta(N))$		$\theta(1)$	$\theta(2)$	$\theta(3)$	$\theta(4)$	$\theta(5)$	$\theta(6)$
S	S_T						
1	1	$V2$	$V3$	$V4$	$V5$	$V6$	$V1$
1	0	$V8$	$V7$	$V8$	$V7$	$V8$	$V7$
1	-1	$V6$	$V1$	$V2$	$V3$	$V4$	$V5$
0	1	$V3$	$V4$	$V5$	$V6$	$V1$	$V2$
0	0	$V7$	$V8$	$V7$	$V8$	$V7$	$V8$
0	-1	$V5$	$V6$	$V1$	$V2$	$V3$	$V4$

Table 3: Voltage vector selection based on reference flux and torque demand

In the "K" Sector	Increase	Decrease
Stator Flux	K, K+1, K-1	K+2, K-2, K+3
Torque	K+1, K+2	K-1, K-2

$$Vs = \sqrt{\frac{2}{3}} V_{dc}\left[V_a + V_b \exp\left(j\frac{2\pi}{3}\right) + V_c \exp\left(j\frac{4\pi}{3}\right)\right], \tag{11}$$

where V_a, V_b, V_c are the instantaneous values of the primary line to neutral voltage. If the switch is at state '0' that means the phase is connected to the negative, if it is at '1' it means that the phase connected to the positive leg respectively. With two level inverter, eight (23) possible switching states are obtained out of which two are inactive states and six are active states.

The three phase two level voltage source inverter is modelled as shown in Fig. 6. Where S_a, S_b, S_c are switching states. Eight output voltage vectors v_1 to v_8 (100,110,010,011,001,101,000,111) are obtained for different switch combinations; v_7 and v_8 are zero voltage vectors. From Tab. 2 based on the combinations of torque error, flux error and sector position corresponding voltage vector is obtained which is fed to the inverter. The machine voltages corresponding to the switching states, inverter voltages are calculated by using the following relations.

$$\left.\begin{aligned} v_{ab} &= v_a - v_b \\ v_{bc} &= v_b - v_c \\ v_{ca} &= v_c - v_a \end{aligned}\right\}. \tag{12}$$

From Eq. (13) the machine phase voltages for a balanced system, from Eq. (14) q and d axes voltages are calculated

$$\left.\begin{aligned} v_{as} &= \frac{v_{ab} - v_{ca}}{3} \\ v_{bs} &= \frac{v_{bc} - v_{ab}}{3} \\ v_{cs} &= \frac{v_{ca} - v_{bc}}{3} \end{aligned}\right\}, \tag{13}$$

$$\left.\begin{aligned} v_{qs} &= v_{as} \\ v_{ds} &= \tfrac{1}{\sqrt{3}}\left(v_{cs} - v_{bs}\right) = \tfrac{1}{\sqrt{3}} v_{cb} \end{aligned}\right\}. \tag{14}$$

3.7 Design of fuzzy logic controller

The general block diagram of FLC is shown in Fig. 6. Fuzzy logic control consists of fuzzification process, linguistic rule base, and defuzzification process.

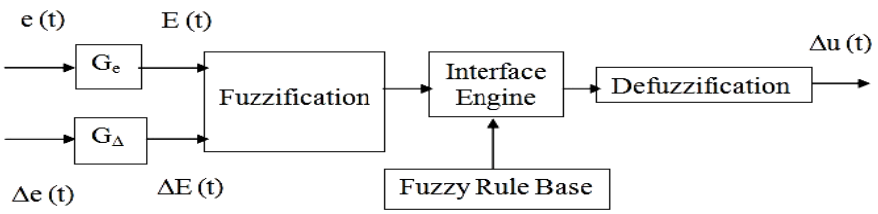

Fig. 6: Block diagram of FLC

Selecting input and output variables in terms of linguistic variable are very much necessary in designing a FLC. After choosing linguistic variables, selection of scaling factors plays a vital role to extract control input to the plant. Among three FLCs (Mamdani, Sugeno, Tsukamoto), Mamdani type fuzzy inference system is considered in this work.

The complete fuzzy rule base matrix (Mamdani type fuzzy inference) is represented in Tab. 4. For the proposed drive performance to obtain the optimum switching logic the values of the constants, membership functions, fuzzy sets for the input-output variables and the rules used are selected by trial and error.

Table 4: Rule Base Table

	$\Delta\omega e$					
	NH	NL	ZE	PL	PH	
	NE	NH	NL	NC	PM	PH
ωe	ZE	NH	NL	NC	PM	PH
	PS	NH	NL	PL	PM	PH

The membership functions are selected such a way to reduce the computational time of the controller (example: The membership function employed is same for Negative Large, Positive Large, Negative and Positive of input vectors) in the proposed FLC.

The FLC is designed for speed control of a PMSM drive system. Hence the input variables for FLC are speed error and change of speed error which are expressed in Eqs. (15) and (16) respectively.

$$e(k) = \omega(k)^* - \omega(k), \tag{15}$$

$$\Delta e(k) = e(k) - e(k-1). \tag{16}$$

The two input variables $e(k)$, $\Delta e(k)$ and output variable command torque (T_ε^*) are divided into different fuzzy segments shown in Figs. 7, 8 and 9 respectively.

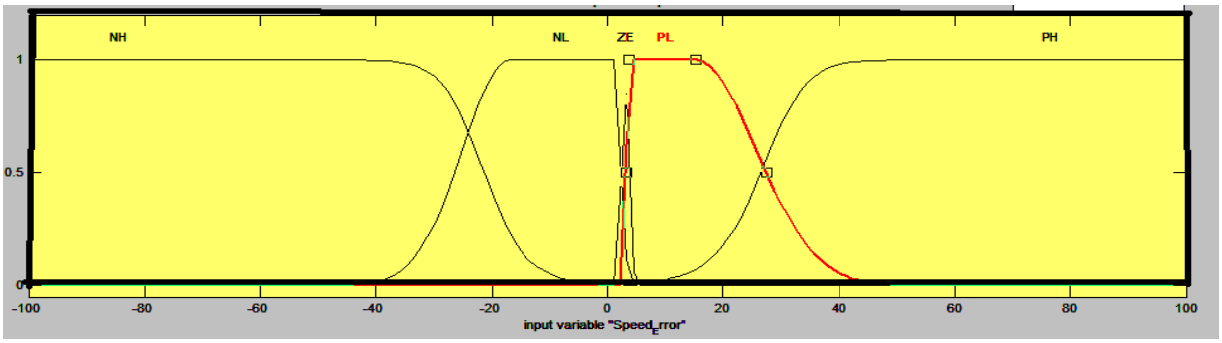

Fig. 7: Membership function for speed error

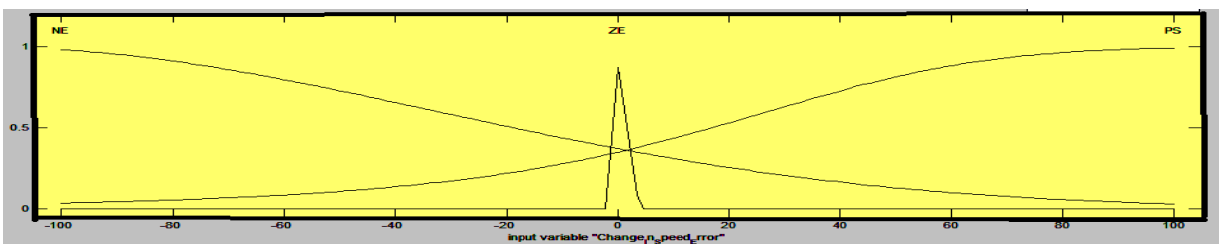

Fig. 8: Membership function for change in speed error

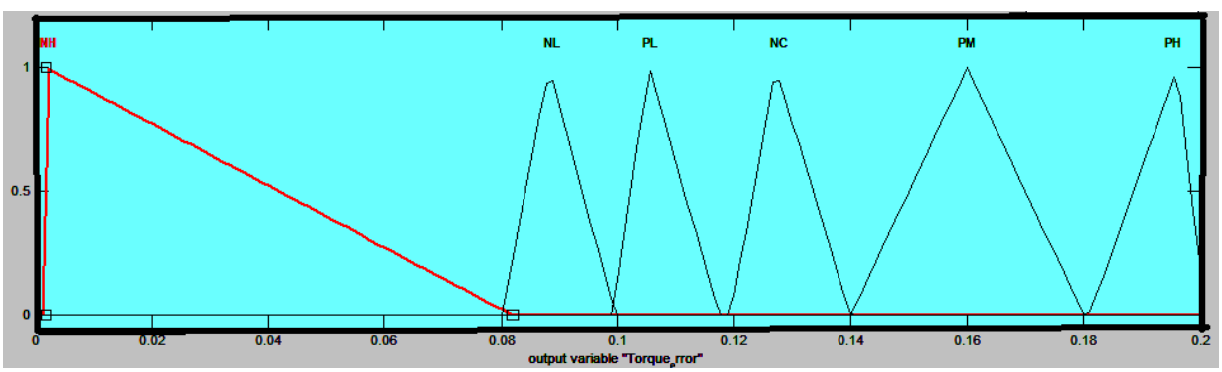

Fig. 9: Membership function for Electromagnetic Torque

For example the rules used for the proposed FLC algorithms are as follows:
(i) If $\Delta\omega_t$ is ZE (Zero) and ω_r is PS (Positive Small) ΔT_ε is PL (Positive Low).
(ii) If $\Delta\omega_r$ is ZE (Zero) and ω_r is ZE (Zero) ΔT_ε is NC (No change) and so on.

3.8 Dynamic performance of DTC for IPM using PI and fuzzy controller

The simulated responses of IPM with PI and Fuzzy controllers are shown from Fig. 10 to Fig. 15 with the proposed DTC (DTC I).From these figures, one can observe that the starting performance as well as the response with a load disturbance.

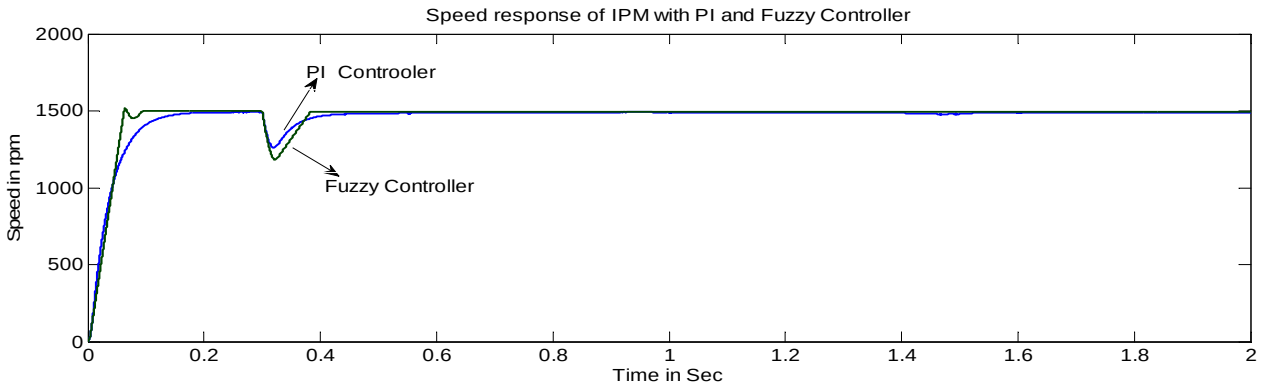

Fig. 10: Speed response of IPM at no load and when load applied at $t = 0.3$ sec with MDTC

In Fig. 10 the drive system is started at no load condition with the speed reference set at 1500 rpm. It is seen from Fig m that the proposed drive with FLC can follow the command speed within 0.08 sec without any over shoot, under shoot and steady state error. Whereas PI controller takes a long time to reach the steady state. At $t = 0.3$ sec, a load torque of 1.95 N/m is applied to the motor shaft in a step wise manner. In both the controllers the speed momentarily follows with load disturbances and immediately within no time reaches to the reference value. However with Fuzzy controller the drive reaches to the reference value faster than with PI controller.

Fig. 10 gives the torque responses of IPM at no load and when load applied at state $t = 0.3$ sec. The steady error is less for the drive with FLC than PI Controller. It is very well illustrated from 0.6 sec onwards.

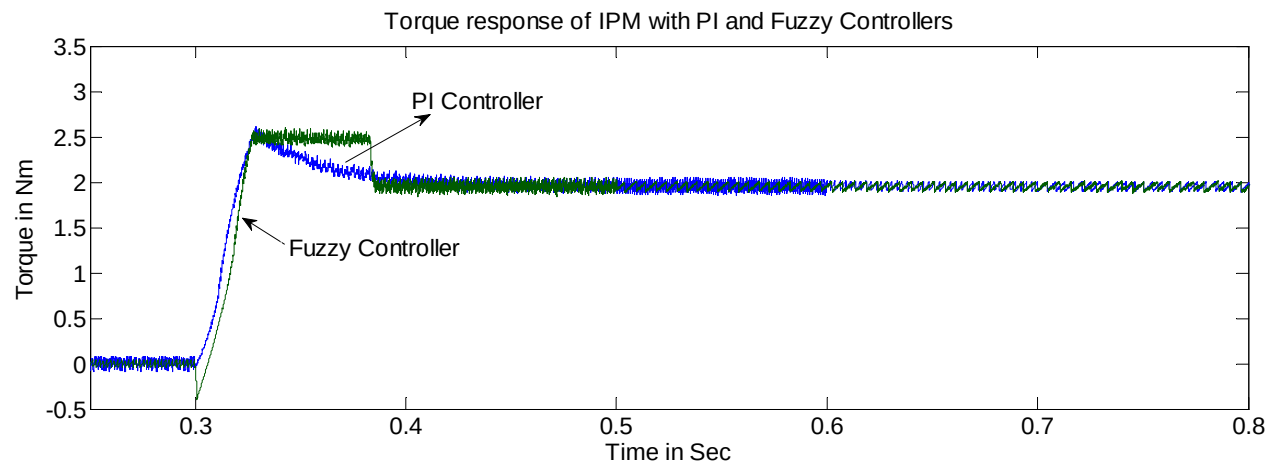

Fig. 11: Torque response of IPM at no load and when load applied at $t = 0.3$ sec with MDTC

Fig. 11 describes the torque and speed responses of IPM with constant load and variable set speeds. When speed is varying from 500 rpm to 1000 rpm at $t = 1$ sec, the dynamic response of speed is faster and smooth with FLC. The steady state speed error is also less with FLC than PI controller. Moreover the torque response possesses more fluctuations with PI controller.

Fig. 13 illustrates the torque and speed response of IPM with constant speed and variable load torques. When load is varying from 0.5 Nm to 1.95 Nm at $t = 1$ sec and 1.95 Nm to 2.5 Nm at $t = 2$ sec; the speed response is smooth with FLC. The steady state error of torque response fluctuates more with PI controller.

From Fig. 14 the torque ripple analysis for IPM is observed with two controllers. The magnitude of torque ripples is more and significant with PI controller. Whereas the torque ripples are smooth by using FLC. Fig. 15 depicts the flux ripple analysis of the IPM drive.

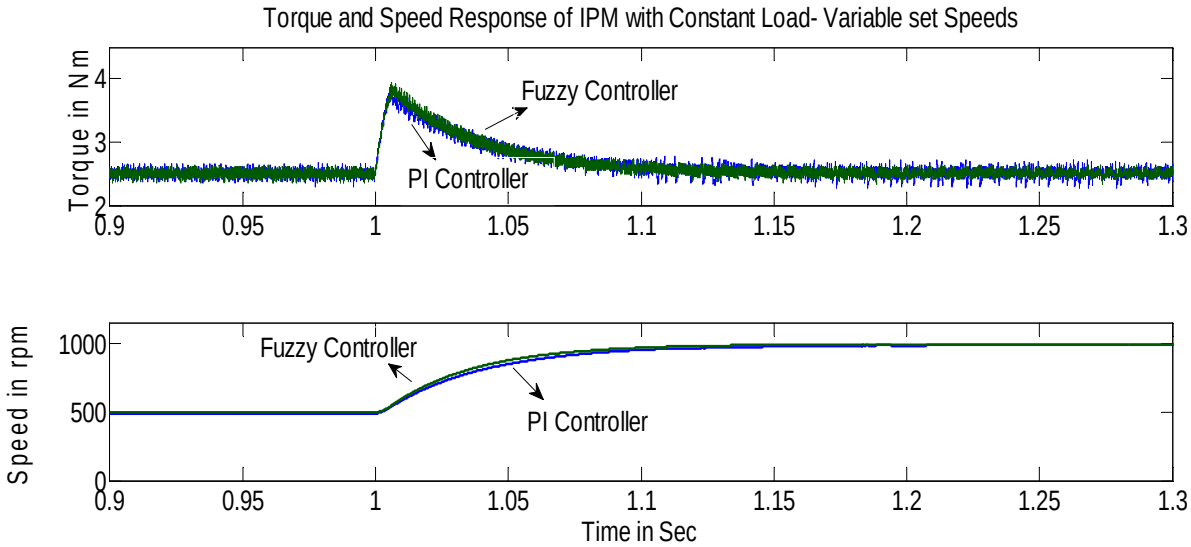

Fig. 12: Speed and torque responses of IPM with constant Load torque and variable set speeds with MDTC

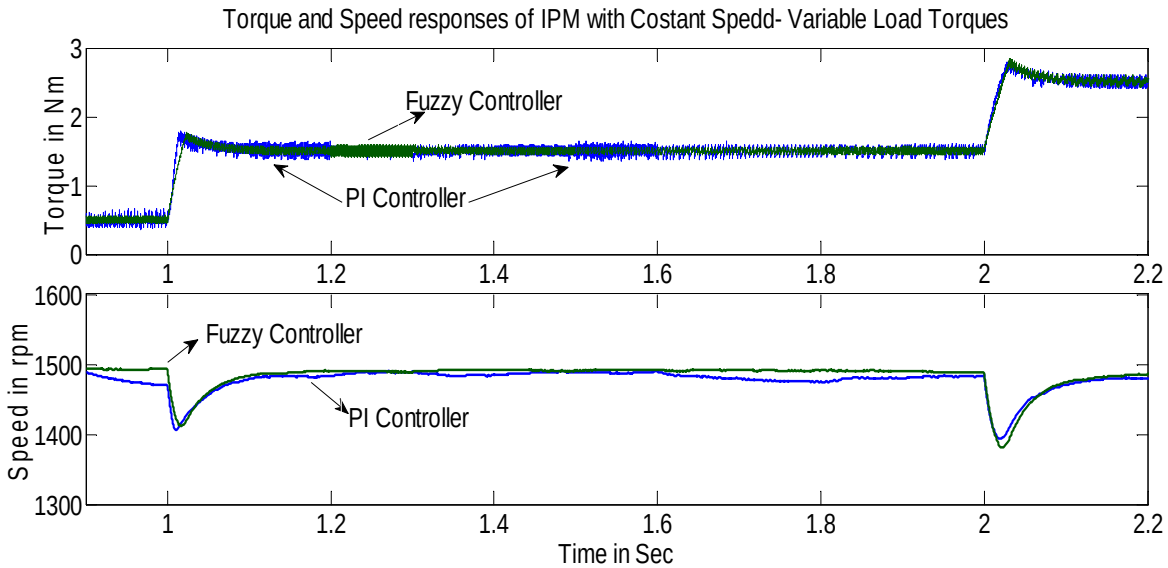

Fig. 13: Speed and torque responses of IPM at constant speed and variable loads with MDTC

The detailed analysis of torque ripples, flux ripple analysis and THD of phase current and voltages are given in Tab. 5 for the following two cases. The specifications of the drive is given in Tab. 6.

(i) $T_L = 1.5$ Nm; Set Speeds 1500rpm and 3000 rpm.

(ii) $T_L = 2.0$ Nm; Set Speeds 1500rpm and 3000 rpm.

4 Performance indices of the system

The proposed PI and FLC based DTC I of IPM and SPM drives has been investigated through simulation. The torque and flux ripples are reduced with FLC compared to PI controller. And the simulation results confirms that the proposed FLC with simple design approach and smaller rule base can provide better performance comparing with the PI controller. Basically the controllers are incorporated for speed response, hence performance indices is carried out for speed response. Tab. 7 illustrates the both rotor configurations of PMSM,

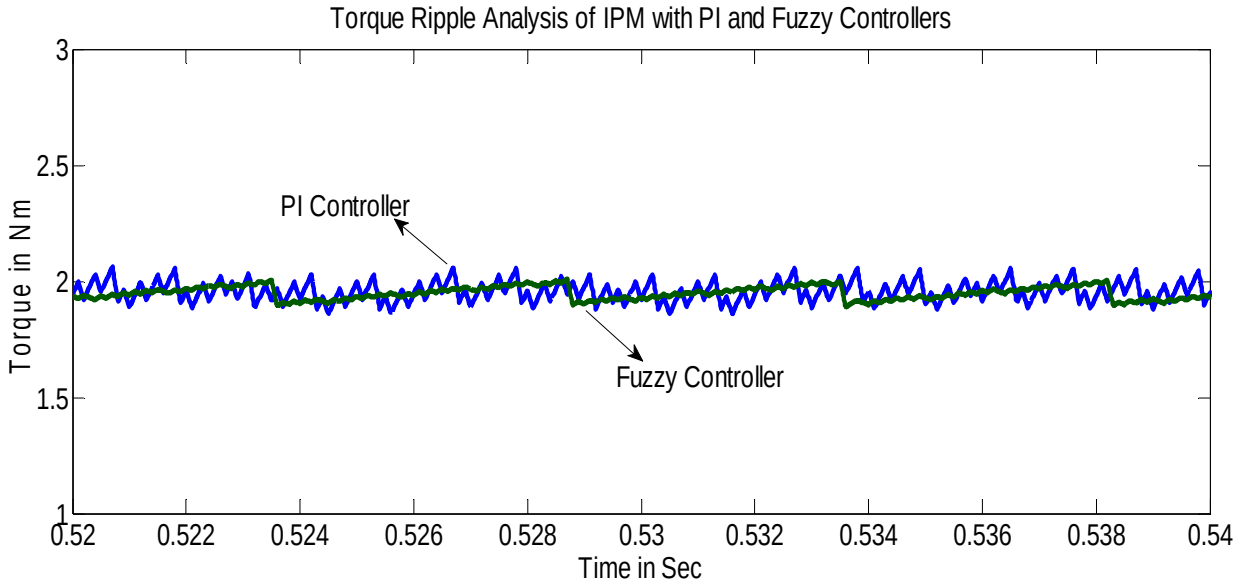

Fig. 14: Comparison of torque ripple analysis of IPM with DTC I

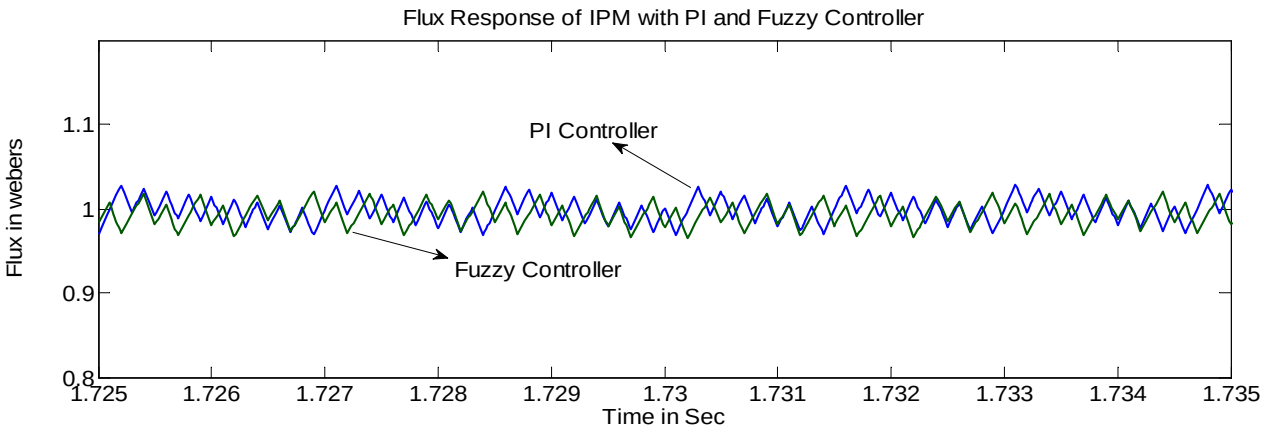

Fig. 15: Comparison of flux ripple analysis of IPM with DTC I

Table 5: Torque Ripple, Flux Ripple and THD of Phase Current Analysis of IPM for MDTC using PI and Fuzzy Controllers

Load Torque (Nm)	Speed (rpm)	Torque Ripple (%)		Flux Ripple (%)		Phase Current (THD) %	
		PI Controller	Fuzzy Logic Controller	PI Controller	Fuzzy Logic Controller	PI Controller	Fuzzy Logic Controller
1.5	1500	16.21	8.86	15.71	11.63	3.43	1.58
	3000	21.49	15.0	9.82	6.45	5.78	2.63
2.0	1500	12.38	5.43	13.59	4.3	3.21	1.22
	3000	15.74	11.32	12.79	10.33	4.62	2.63

drive performance is better with FLC than PI Controller. Figs. 16, 17, 18 and 19 confirms this statement for SPM drive.

5 Conclusion

MDTC is adopted to minimize the torque ripples of a IPMSM. The flux and torque are controlled efficiently by appropriate selection of the voltage vector. The flux and torque hysteresis controllers decide the

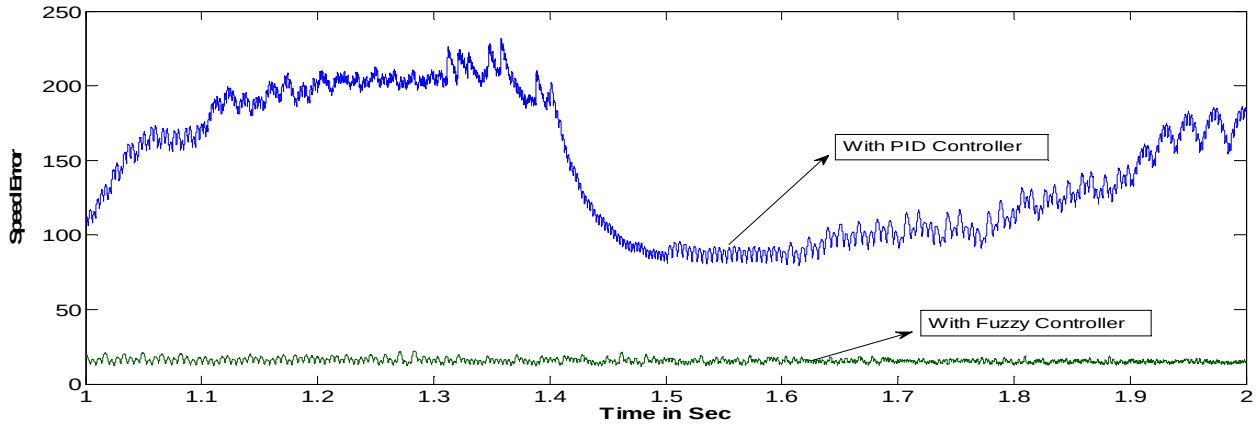

Fig. 16: Integral of squared error (ISE) with PI and fuzzy controllers

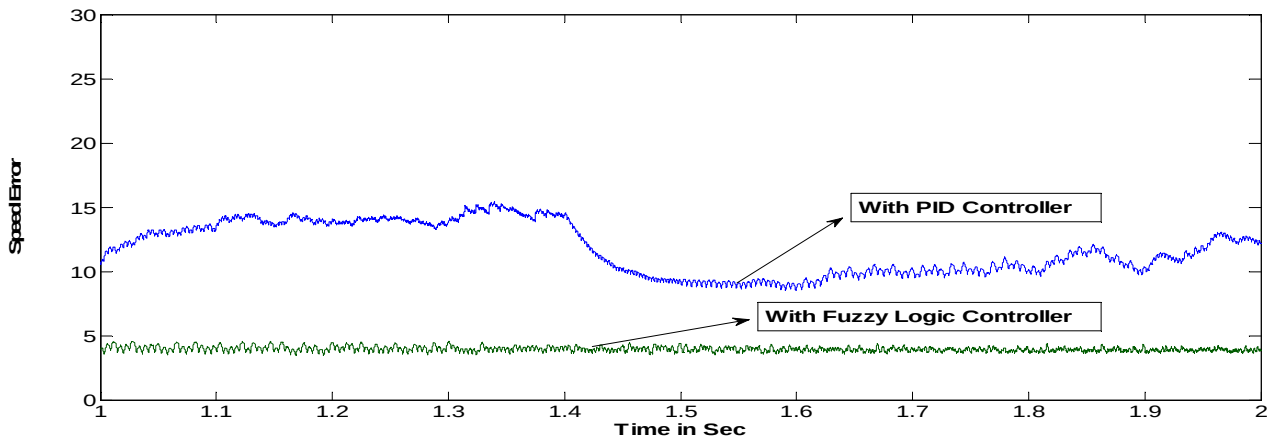

Fig. 17: Integral of absolute error (IAE) with PI and fuzzy controllers

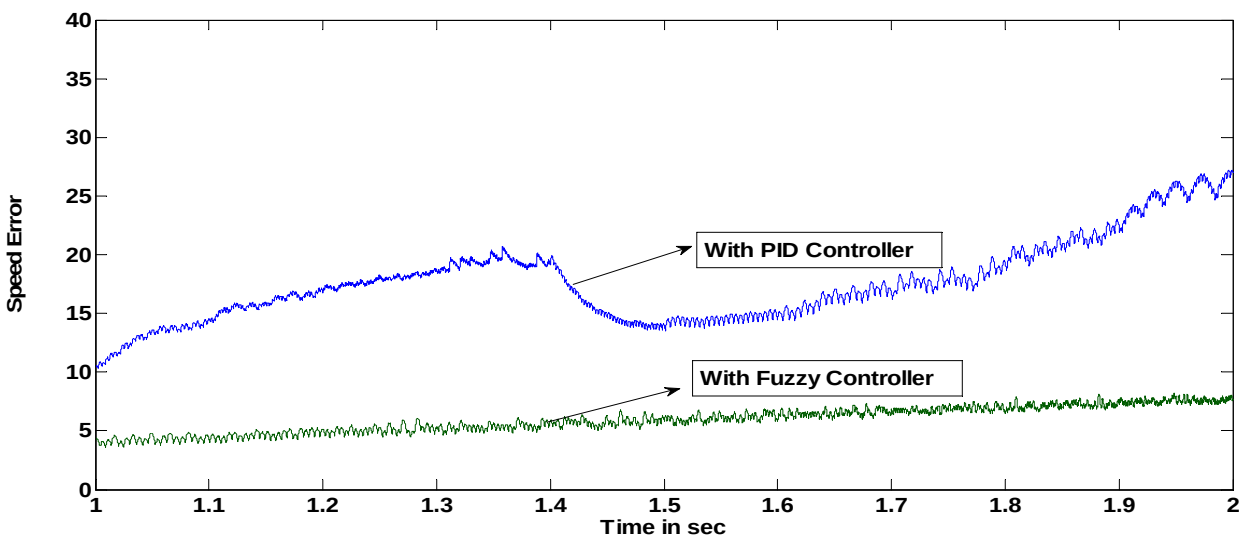

Fig. 18: Integral of time multiply squared error (ITSE) with PI and fuzzy controllers

Table 6: Parameters of the IPMSM

Number of pole pairs	p	2
Stator resistance	R_s	19.4 Ω
Magnetic flux linkage	λ_f	0.477 Wb
d-axis inductance	L_d	0.3875 H
q-axis inductance	L_q	0.4755 H
Phase voltage	V	145 V
Phase current	I	3 A
Base speed	ω_b	1500 rpm
Rated torque	T_b	1.95 Nm
Moment of Inertia	J	3.8e^{-3}Kg/m^2
Viscous Coefficient	B	1e^{-5}
DC link Voltage	Vdc	848 V
Reference Flux	λ	1.7 Wb

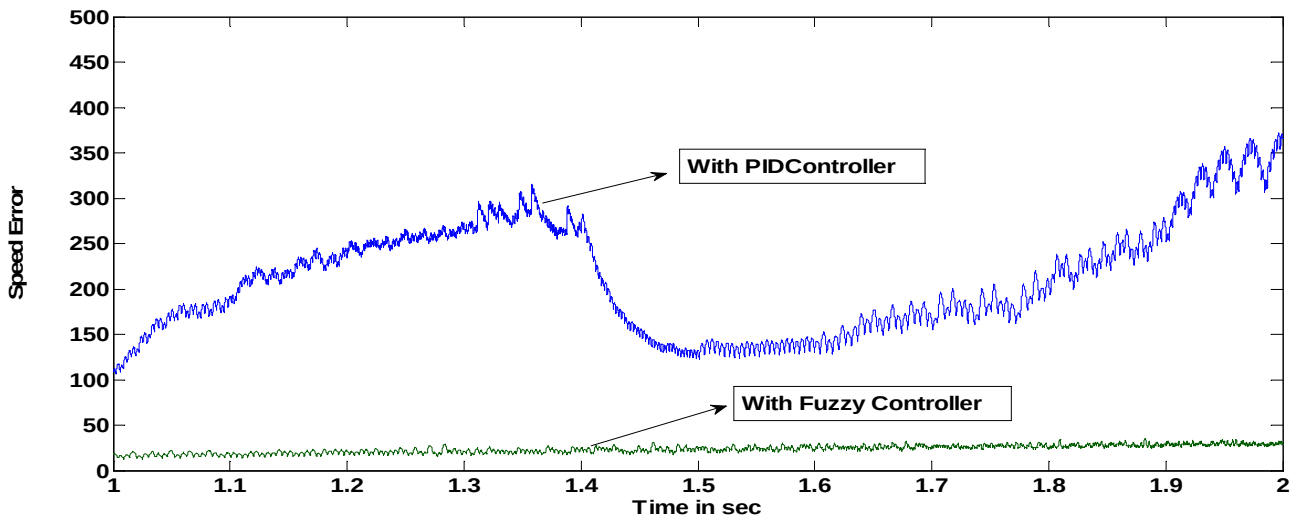

Fig. 19: Integral of time multiply absolute error (ITAE) with PI and fuzzy controllers

Table 7: Performance indices of the system–SPM

Performance Indices	IPM	
	Magnitude of Speed Error With PI Controller	Magnitude of Speed Error With FLC
ISE	1.5	0.15
IAE	0,12	0.04
ITSE	3	0.3
IATE	0.27	0.06

band width of the flux and torque. It is preferable to have a smaller sampling interval to have a smaller band width for hysteresis controllers which controls the stator flux more precisely. So in order to increase the performance of a drive small control periods must be selected. Also the calculation of DC voltage is important to keep the flux out of saturation.

In DTC, appropriate voltage space vector with less hysteresis band are very much necessary to attain an exact control of torque and flux linkages. Since DTC do not offer proper mathematical outcome with a usual controllers like PI, it is necessary to use FLC.

It is noticed that the torque and flux ripples are reduced with FLC. Also the results confirm that the proposed FLC with simple design approach and smaller rule base can provide better performance comparing with the PI controller which is very well proved from the performance indices of the system.

From observations it is noticed that for steady state analysis PI controller and for transient analysis FLC is recommended. Also for non linear systems FLC gives better performance than PID which is evident from the analysis of performance indices.

References

[1] L. Antal, P. Zalas. Soft and synchronous starting of low-power smpmsm motor. *Philosophy Now*, 2013.

[2] K. Boughrara, D. Zarko, et al. Magnetic field analysis of inset and surface-mounted permanent-magnet synchronous motors using schwarz-christoffel transformation. *IEEE Transactions on Magnetics*, 2009, **45**(8): 3166–3178.

[3] P. Brandstetter, P. Chlebis, P. Palacky. Direct torque control of induction motor with direct calculation of voltage vector. *Advances in Electrical & Computer Engineering*, 2010, **10**(4): 17–22.

[4] J. J. Chen, K. P. Chin. Minimum copper loss flux-weakening control of surface mounted permanent magnet synchronous motors. *IEEE Transactions on Power Electronics*, 2003, **18**(4): 929–936.

[5] A. Faggion, N. Bianchi, S. Bolognani. Ringed-pole permanent-magnet synchronous motor for position sensorless drives. *IEEE Transactions on Industry Applications*, 2011, **47**(4): 1759–1766.

[6] C. French, P. Acarnley. Direct torque control of permanent magnet drives. *IEEE Trans on Industrial Applications*, 2015, **32**(5): 1080–1088.

[7] X. D. T. Garcia, B. Zigmund, et al. Comparison between FOC and DTC strategies for permanent magnet synchronous motors. *Advances in Electrical & Electronic Engineering*, 2006, **5**(1 - 2): 76–81.

[8] Y. S. Kung, M. H. Tsai. Fpga-based speed control ic for pmsm drive with adaptive fuzzy control. *IEEE Transactions on Power Electronics*, 2007, **22**(6): 2476–2486.

[9] T. S. Kwon, S. K. Sul. Novel anti-windup of a current regulator of a surface-mounted permanent-magnet motor for flux-weakening control. *Industry Applications IEEE Transactions on*, 2006, **42**(5): 1813–1819 Vol. 3.

[10] P. Y. Lin, Y. S. Lai. Voltage control technique for the extension of DC-link voltage utilization of finite-speed SPMSM drives. *IEEE Transactions on Industrial Electronics*, 2012, **59**(9): 3392–3402.

[11] C. Mademlis, J. Xypteras, N. Margaris. Loss minimization in surface permanent-magnet synchronous motor drives. *IEEE Transactions on Industrial Electronics*, 2000, **47**(1): 115–122.

[12] A. Meroufel, A. Massoum, B. Belabes. Fuzzy adaptive model following speed control for vector controlled permanent magnet synchronous motor. *Leonardo Electronic Journal of Practices & Technologies*, 2008, **7**(13).

[13] M. S. Merzoug, F. Naceri. Comparison of field-oriented control and direct torque control for permanent magnet synchronous motor (PMSM). *Proceedings of World Academy of Science Engineering & Technolog*, 2008, (45): 300.

[14] A. Nasiri. Full digital current control of permanent magnet synchronous motors for vehicular applications. *IEEE Transactions on Vehicular Technology*, 2007, **56**(4): 1531–1537.

[15] P. H. Nguyen, E. Hoang, M. Gabsi. Power loss evaluation of a surface mounted permanent magnet synchronous machine during two hybrid electric vehicle driving cycles. *Journal of Asian Electric Vehicles*, 2011, **9**(1): 1465–1471.

[16] A. B. Proca, A. Keyhani, et al. Analytical model for permanent magnet motors with surface mounted magnets. *IEEE Transactions on Energy Conversion*, 2003, **18**(3): 386–391.

[17] R. Qu, T. A. Lipo. Analysis and modeling of air-gap and zigzag leakage fluxes in a surface-mounted permanent-magnet machine. *IEEE Transactions on Industry Applications*, 2004, **40**(1): 121–127.

[18] L. Romeral, J. C. Urresty, et al. Modeling of surface-mounted permanent magnet synchronous motors with stator winding interturn faults. *IEEE Transactions on Industrial Electronics*, 2011, **58**(5): 1576–1585.

[19] G. R. Slemon. On the design of high-performance surface-mounted PM motors. *IEEE Transactions on Industry Applications*, 1994, **30**(1): 134–140.

[20] I. Takahashi, T. Noguchi. A new quick-response and high-efficiency control strategy of an induction motor. *IEEE Transactions on Industry Applications*, 1986, **22**(5): 820 – 827.

[21] L. Tang, L. Zhong, et al. A novel direct torque control for interior permanent-magnet synchronous machine drive with low ripple in torque and flux-a speed-sensorless approach. *IEEE Transactions on Industry Applications*, 2003, **39**(6): 1748–1756.

[22] T. Tudorache, M. Popescu. Optimal design solutions for permanent magnet synchronous machines. *Advances in Electrical & Computer Engineering*, 2011, **11**(4): 77–82.

[23] M. Tursini, E. Chiricozzi, R. Petrella. Feedforward flux-weakening control of surface-mounted permanent-magnet synchronous motors accounting for resistive voltage drop. *IEEE Transactions on Industrial Electronics*, 2010, **57**(1): 440–448.

[24] S. R. Vaishnav, Z. J. Khan. Design and performance of PID and fuzzy logic controller with smaller rule set for higher order system. *Lecture Notes in Engineering & Computer Science*, 2007, **2167**(1).

[25] B. Wang, Y. Wang, Z. Wang. A modified direct torque control of surface permanent magnet synchronous motor drives without a speed sensor. **in:** *Power Electronics and Motion Control Conference, 2009. IEEE 6th International.*, 2009, 1871–1874.

[26] X. Wang, Y. Xing, et al. Research and simulation of DTC based on svpwm of pmsm. *Procedia Engineering*, 2012, **29**(4): 1685–1689.

[27] S.-C. Yang, T. Suzuki, et al. Surface-permanent-magnet synchronous machine design for saliency-tracking self-sensing position estimation at zero and low speeds. *IEEE Transactions on Industry Applications*, 2011, **47**(5): 2103–2116.

[28] L. A. Zadeh. Fuzzy sets. *Information & Control*, 1965, **8**(3): 338–353.

[29] S. Zhao, X. Peng. A modified direct torque control using space vector modulation (DTC-SVM) for surface permanent magnet synchronous machine (PMSM) with modified 4-order sliding mode observer. **in:** *Mechatronics and Automation, 2007. ICMA 2007. International Conference on*, 2007, 1207 – 1212.

[30] L. Zhong, M. F. Rahman, et al. Analysis of direct torque control in permanent magnet synchronous motor drives. *IEEE Transactions on Power Electronics*, 1997, **12**(3): 528–536.

[31] Z. Q. Zhu, D. Howe. Influence of design parameters on cogging torque in permanent magnet machines. *IEEE Transactions on Energy Conversion*, 2001, **15**(4): 407–412.